



## Effect of pion thermal width on the sigma spectrum

Tetsuo Nishikawa<sup>a\*</sup>, Yoshimasa Hidaka<sup>a</sup>, Munehisa Ohtani<sup>b</sup> and Osamu Morimatsu<sup>a</sup>

<sup>a</sup>Institute of Particle and Nuclear Studies, High Energy Accelerator Research Organization, 1-1, Ooho, Tsukuba, Ibaraki, 305-0801, Japan

<sup>b</sup>The Institute of Physical and Chemical Research (RIKEN), 2-1 Hirosawa, Wako, Saitama 351-0198, Japan

We study the effect of the thermal width of  $\pi$  on the spectral function of  $\sigma$ . In order to take into account a finite thermal width of  $\pi$ , we replace the internal pion mass in the self-energy of  $\sigma$  with that of the complex pole found in a previous paper. The obtained spectral function for  $T \gtrsim 100\text{MeV}$  turns out to possess two broad peaks. Although a sharp peak at  $\sigma \rightarrow \pi\pi$  threshold was observed in the one-loop calculation without the pion thermal width, the peak is shown to be smeared out. We also search for the poles of the  $\sigma$  propagator and analyze the behavior of the spectral function with these poles.

Restoration of the chiral symmetry in hot matter has attracted much attention since drastic spectral change of light mesons is expected to be a precursor of the restoration [1]. Physical mechanism of the spectral change is explained with the mass shift of mesons as follows. As the temperature increases to the critical temperature, the mass of  $\sigma$  reduces while light  $\pi$  becomes heavy, because their masses should degenerate after the symmetry restoration. At a certain temperature, therefore, the mass of  $\sigma$  coincides with twice that of  $\pi$ . Accordingly, the spectrum of  $\sigma$  is expected to be enhanced near the threshold of  $\sigma \rightarrow \pi\pi$ , since the phase space available for the decay is squeezed to zero.

Chiku and Hatsuda [2] showed that the threshold enhancement in the  $\sigma$  channel is observed as expected. They also calculated the spectral function of  $\pi$  and found that  $\pi$  has a finite width due to pion absorption in the heat bath:  $\pi + \pi^{\text{thermal}} \rightarrow \sigma$ . The width of  $\pi$  is  $\sim 50\text{MeV}$  at the temperature where the threshold in the  $\sigma$  spectrum is most strongly enhanced. In their analysis of the spectrum of  $\sigma$ , however, the effect of the pion thermal width is not included, since they calculated the self-energy only up to the one-loop order. The purpose of this paper is to show that the threshold enhancement is smeared out by taking into account the effect of the pion thermal width.

Our strategy is as follows. We utilize the one-loop self-energy for  $\sigma$ , but we replace the masses of internal pions with complex ones. This complex mass was obtained from the location of the pole of the pion propagator in a previous work [3]. Using the self-energy with the complex pion mass, we study the spectral function of  $\sigma$ . The poles of the  $\sigma$  propagator are also searched for to analyze the behavior of the spectral function.

Along the lines mentioned above, here we employ the  $\mathcal{O}(4)$  linear sigma model. It is known that naive perturbation theory breaks down at  $T \neq 0$ , and resummation of higher or-

ders is necessary. We adopt here a resummation technique called optimized perturbation theory (OPT) [2]. In OPT one adds and subtracts a new mass term with the mass  $m$  to the Lagrangian. One treats the added one as a tree-level mass term while the subtracted one as perturbation. The arbitrary parameter  $m$  is determined so that the correction terms in the pion self-energy are as small as possible [2].

The effects of the pion thermal width on the spectrum of  $\sigma$  are included in the self-energy at the two or higher loop level. The two-loop self-energy gives vertex corrections, mass shifts and thermal widths of  $\sigma$  and  $\pi$ . Among them, the pion thermal width is the most important as an effect beyond the one-loop calculation, from the reason explained in the next paragraph.

Although several processes contribute to the two-loop self-energy, the most relevant process is the pion scattering,  $\sigma\pi^{\text{thermal}} \rightarrow \sigma\pi$ , because  $\pi$  is the lightest in the heat bath and we concentrate on the energy region near the  $\pi\pi$  threshold. This process contributes to the imaginary part of the two-loop self-energy in the following way;

$$\begin{aligned} \text{Im}\Pi_{\sigma}^{2\text{-loop}}(k, T) &\sim \int \frac{d^3p}{(2\pi)^3} \frac{1}{2\omega_{\pi}} \frac{d^3p'}{(2\pi)^3} \frac{1}{2\omega_{\sigma}} \frac{d^3k'}{(2\pi)^3} \frac{1}{2\omega_{\pi}} \\ &\times (2\pi)^4 \delta^{(4)}(p+k-p'-k') |\mathcal{M}_{\sigma\pi \rightarrow \sigma\pi}|^2 \\ &\times \{n_{\pi}(1+n_{\sigma})(1+n_{\pi}) - (1+n_{\pi})n_{\sigma}n_{\pi}\}, \end{aligned} \quad (1)$$

where  $n_{\phi}$  is a thermal factor and  $\mathcal{M}_{\sigma\pi \rightarrow \sigma\pi}$  the amplitude of  $\sigma\pi^{\text{thermal}} \rightarrow \sigma\pi$ . The tree-level amplitude of the scattering is shown in Fig.1 and written as

$$\begin{aligned} \mathcal{M}_{\sigma\pi \rightarrow \sigma\pi} &= \frac{-i\lambda}{3} + \frac{-\lambda^2\xi^2}{9} \left[ \frac{i}{(k+p)^2 - m_{0\pi}^2} \right. \\ &\quad \left. + \frac{i}{(k-p')^2 - m_{0\pi}^2} + \frac{3i}{(k-k')^2 - m_{0\sigma}^2} \right], \end{aligned} \quad (2)$$

where  $m_{0\phi}$  is the tree level mass. If  $k^2 = m_{0\sigma}^2$ ,  $\mathbf{p}, \mathbf{k} \rightarrow 0$ , and  $m_{0\sigma} \gg m_{0\pi}$ , four terms in Eq. (10) cancel out due to the

\*Speaker at the Workshop.

chiral symmetry. However we are interested in the spectral function  $\rho_\sigma(k, T)$  for  $k_0 \equiv \omega \simeq 2m_{0\pi}$ , and therefore the third term is dominant;

$$\begin{aligned} \mathcal{M}_{\sigma\pi \rightarrow \sigma\pi} &= -i\frac{\lambda}{3} \left\{ 1 + (m_{0\sigma}^2 - m_{0\pi}^2) \left[ \frac{1}{\omega(\omega + 2m_{0\pi})} \right. \right. \\ &\quad \left. \left. + \frac{1}{\omega(\omega - 2m_{0\pi})} + \frac{1}{\omega(\omega - 2m_{0\sigma})} \right] \right\} \\ &\simeq -i\frac{\lambda}{3} \frac{1}{\omega(\omega - 2m_{0\pi})}. \end{aligned} \quad (3)$$

This term comes from the cut diagram shown in Fig.2. This fact indicates that a correction for the self-energy of  $\pi$  is the most important contribution for the sigma spectrum beyond the one-loop level. Higher order corrections as shown in Fig.2 are also large. Therefore, it is necessary to resum at least higher order corrections of this class of diagrams. This resummation can be performed by replacing the internal pion propagators of  $\Pi_\sigma$  with the pion propagators in the one-loop level. Instead of using the complicated pion propagator in the one-loop level, we adopt here a simplified prescription — to use a complex pion pole as internal pion mass in  $\Pi_\sigma$ , in order to include the most important effect. The thermal width of  $\pi$  is represented as the imaginary part of the complex pole of the pion propagator:

$$p^2 - m_{0\pi}^2 - \Pi_\pi(p^2, p; T) \Big|_{p^2=(m_\pi^{\text{pole}})^2} = 0, \quad (4)$$

$$m_\pi^{\text{pole}} = m_\pi^*(T) - i\frac{\Gamma_\pi(T)}{2}, \quad (5)$$

where  $\Pi_\pi$  is the one-loop pion self-energy [ 3].

As a matter of course, the pole has a dependence on  $|p|$  naturally [ 3], but contributions from  $|p| \gtrsim T$  are less effective to the loop integration in the thermal part of  $\Pi_\sigma$ . Therefore, as a simple prescription to incorporate the thermal width, we replace the internal pion mass,  $m_{0\pi}$ , in the one-loop self-energy with  $m_\pi^{\text{pole}}$  at  $p = \mathbf{0}$  in Ref.[ 3] as depicted in Fig.3 to obtain the spectral function  $\rho_\sigma$ .

We show in Fig.4 the obtained spectral function at  $k = \mathbf{0}$  for several values of  $T$ . For comparison, we also show the spectral function at  $T = 145\text{MeV}$  with  $m_{0\pi}$  and that

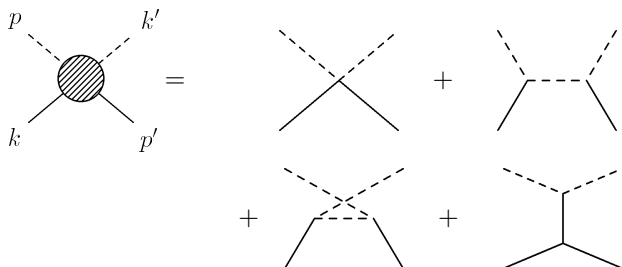


**Figure 1.** The scattering amplitude of  $\sigma\pi \rightarrow \sigma\pi$  at lowest order.

with  $m_\pi^{\text{pole}}$  in Fig.5. At low  $T$  the spectrum consists of a broad bump around  $\omega = 550\text{MeV}$ . As  $T$  increases, another strength grows at the left shoulder of the bump, while the spectrum for  $\omega \gtrsim 400\text{MeV}$  does not vary much. In contrast to this case, if  $m_{0\pi}$  is used as the internal pion mass, the spectrum near the threshold of  $\sigma \rightarrow \pi\pi$  is enhanced as  $T$  is increased. At  $T = 145\text{MeV}$ , where the mass of  $\sigma$  coincides with  $2m_{0\pi}$ , the spectrum near the threshold is most strongly enhanced as shown in Fig.5 (dotted curve). When  $m_\pi^{\text{pole}}$  is used, however, due to the thermal width of  $\pi$  in the decay  $\sigma \rightarrow \pi\pi$ , the sharp threshold is smeared to be a bump at  $\omega = 200\text{MeV} \sim 300\text{MeV}$  as the solid curve in Fig.5.

In general, the behavior of the spectral function is governed by poles of the propagator. We thus next search the complex  $\omega$  plane for the poles of the propagator. The analytic structure of the propagator is determined by that of the self-energy. Then, we see that the self-energy has a branch point at  $\omega = 2m_\pi^{\text{pole}}$  around which the Riemann sheet is two-fold. The self-energy has another branch point due to the  $\sigma$  loop which, however, is irrelevant for the present discussion of the self-energy around the threshold of  $\sigma \rightarrow \pi\pi$ . This is because the branch point risen from the  $\sigma$  loop is located at the twice of the  $\sigma$  mass, which is far from the  $\pi\pi$  threshold even if  $\rho_\sigma$  has some strength below the threshold. The branch cut from  $\omega = 2m_\pi^{\text{pole}}$  can be arbitrarily chosen at finite temperature, because it has no physical meaning. For definiteness we choose the cut from the branch point straight to the right, parallel to the real axis and refer to the sheet including the physical real energy as the first Riemann sheet and the other one as the second Riemann sheet. We show in Fig.6 the result of searching the locations of the poles on the Riemann sheets.

We found three relevant poles. Two of them, (II) and (II\*), are on the second Riemann sheet and off the real axis. Their positions are approximately symmetric with respect to the real axis with each other. For the spectral function of  $\sigma$ , on one hand, (II) and (II\*) show up as a bump around  $\omega = 550\text{MeV}$  and the small movement of these poles explains the insensitivity to  $T$  of the spectrum for  $\omega \gtrsim 400\text{MeV}$ . On the other hand, the structure of the spectrum for low  $\omega$  is mainly determined by the remaining one pole, (I). For preparation to consider this pole (I), let us first recall the movement of the corresponding pole in case of no thermal width of  $\pi$  [ 3].

Without the pion width, the counterpart of the pole (I) ex-

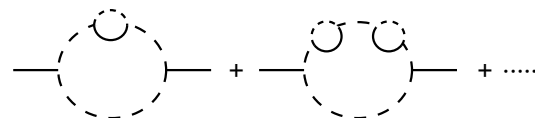


**Figure 2.** The higher-loop self-energies responsible for the thermal width of  $\pi$  from the decay  $\sigma \rightarrow \pi\pi$ .

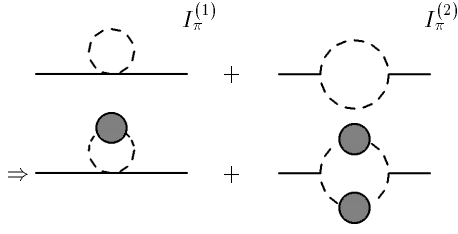


**Figure 3.** A Prescription to take into account the thermal width of  $\pi$  in the decay  $\sigma \rightarrow \pi\pi$ . The upper diagrams represent the self-energy of with the internal pion mass,  $m_{0\pi}$ , and the lower diagrams with  $m_{\pi}^{\text{pole}}$ .

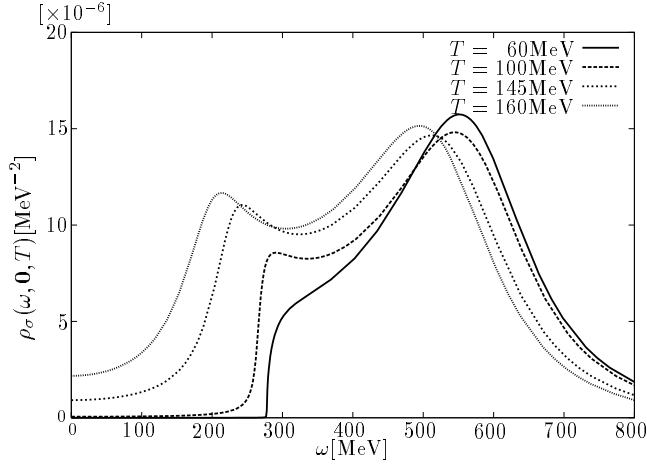


**Figure 4.** Spectral function of  $\sigma$  with the thermal width of  $\pi$ .

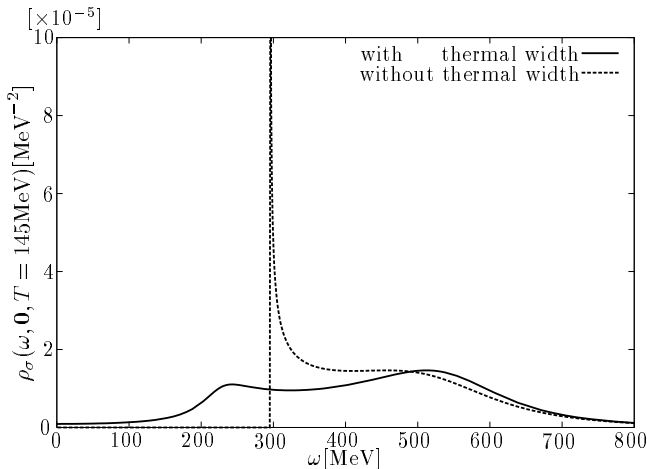


**Figure 5.** Spectral function of  $\sigma$  with and without the thermal width of  $\pi$  at  $T = 145 \text{ MeV}$ .

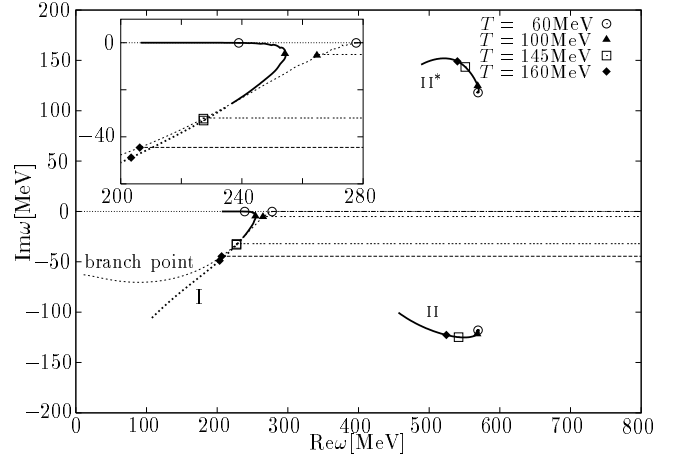


**Figure 6.** Location of the poles of the  $\sigma$  propagator with the thermal width of  $\pi$ ,  $m_{\sigma}^{\text{pole}}$ . The branch point is shown by dotted line and the branch cut are also indicated. We enlarge the figure near the branch point and show it in the inserted box.

ists on the second Riemann sheet apart from the branch point of  $2m_{0\pi}$  for  $T \lesssim 60 \text{ MeV}$ . Correspondingly, the  $\sigma$  spectrum has no peak at the  $\pi\pi$  threshold for low  $T$ . As  $T$  increases, the pole moves along the real axis from below toward the branch point  $2m_{0\pi}$  and turns around at the point to appear on the first sheet at  $T = 145 \text{ MeV}$ . In response to this movement, the  $\sigma$  spectrum is strongly enhanced for  $T \sim 145 \text{ MeV}$ . In other words, the threshold enhancement originates in the fact that the  $\sigma$  pole approaches the branch point on the real axis near the temperature concerned.

Keeping this in mind, we return to the discussion on movement of the pole (I) next. As is the case with no pion width, this pole also resides on the second Riemann sheet for low  $T$  and comes closer to the branch point with increasing  $T$  as shown in Fig.6. At  $T = 138 \text{ MeV}$ , the pole crosses the branch cut and appears on the first Riemann sheet from the second, likewise. The branch point, however, is located at  $2m_{\pi}^{\text{pole}}$  apart from the real axis for  $T \gtrsim 100 \text{ MeV}$  due to the finite thermal width of  $\pi$  (see Fig.6). The complex branch point demands that the pole (I), whose counterpart caused the threshold enhancement by moving toward the point, also acquires an imaginary part near  $T \sim 138 \text{ MeV}$ . As a result, the  $\sigma$  spectrum is smeared and the remarkable contrast is brought about for the spectrums as shown in Fig.5.

Let us argue on the correlation between the spectral function and poles of the propagator more quantitatively. For this purpose, we approximate the propagator of  $\sigma$  with the superposition of the three pole contributions in the following way:

$$\rho_{\sigma} \simeq -2\text{Im} \sum_{\text{pole}} \frac{Z^{\text{pole}}}{q - q_{\text{pole}}},$$

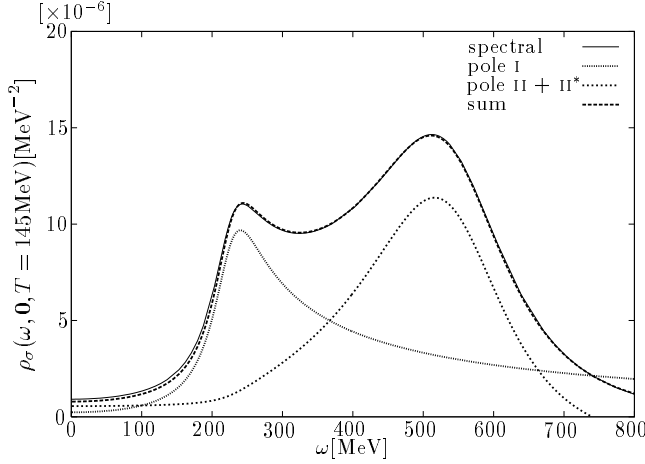


**Figure 7.** The spectral function approximated by a superposition of the contributions from the three poles, Eq.(6), at  $T = 145$  MeV.

$$Z^{\text{pole}} = \frac{1}{2q_{\text{pole}}} \left( 1 - \frac{\partial \Pi_{\sigma}}{\partial k^2} (k^2 = (m_{\sigma}^{\text{pole}})^2) \right)^{-1}, \quad (6)$$

where  $m_{\sigma}^{\text{pole}}$  stands for the pole of the  $\sigma$  propagator.  $q$  and  $q_{\text{pole}}$  are defined by  $q = (k^2 - (2m_{\pi}^{\text{pole}})^2)^{1/2}$  and  $q_{\text{pole}} = ((m_{\sigma}^{\text{pole}})^2 - (2m_{\pi}^{\text{pole}})^2)^{1/2}$ , respectively. It should be noted that we have taken not  $k^2$  but  $q = (k^2 - (2m_{\pi}^{\text{pole}})^2)^{1/2}$  as an appropriate variable. The use of this variable enables us to unfold two leaves of the Riemann sheet around the branch point [5]; We can reflect which Riemann sheet accommodates each pole on the approximated propagator. We show the approximated spectral function, Eq.(6), for one case,  $T = 145$  MeV, in 7. At  $T = 60$  MeV, the pole (I) is located on the second Riemann sheet, while it is on the first sheet at  $T = 145$  MeV. We can see that the poles (II) and (II\*) provide the broad peak around  $\omega = 550$  MeV and that the pole (I) mainly determines the behavior of the left shoulder of the peak. If we include only the contributions of (I) and (II), two broad peaks are still reproduced. However, a structure which is not seen in the spectral function appears at low  $\omega$  region. The contribution of (II\*) cancels out the spurious structure caused by (II). At  $T = 60$  MeV, the left shoulder of the peak is small, although the pole (I) seems to lie close to the real axis. This is because the pole is on the second Riemann sheet and is practically far from the real axis. In contrast, at  $T = 145$  MeV, the pole (I) is on the first Riemann sheet and is close to the real axis. Accordingly, it provides a peak with more strength around  $\omega = 200 \sim 300$  MeV. Thus, in order to reveal the relation between the poles and the behavior of the spectrum, it is necessary to know both of the complex structure of the Riemann sheet and the positions of the poles on it.

Before concluding this paper, a comment on the complex-pole approximation is in order. As, we have shown above, the behavior of the pole of the sigma propagator in the

complex energy plane, which determines the smearing of the sigma threshold strength, is essentially governed by the branch point of the sigma self-energy. And the branch point of the self-energy is correctly given by the complex-pole approximation. Therefore, the results of the present paper are expected to be basically intact beyond the complex-pole approximation.

In conclusion, the thermal width of  $\pi$  smears out the sharp peak of the  $\sigma$  spectrum at  $\pi\pi$  threshold. The structure of the spectral function can be well understood from the three relevant poles of the propagators and the branch points of the self-energy. Physically we can interpret the origin of the smearing as follows. By replacing the masses of  $\pi$  in the decay  $\sigma \rightarrow \pi\pi$  with the complex mass, processes like  $\sigma\pi^{\text{thermal}} \rightarrow \sigma\pi$  are newly taken into account. Since this process is allowed for any energy of the initial  $\sigma$  [6],  $\pi\pi$  threshold disappears thereby. Due to the above process, the  $\sigma$  peak at the threshold is expected to acquire a width of

$$\Gamma_{\sigma} \sim n_{\pi} \cdot \sigma_{\pi\sigma} \cdot m_{\pi}^3 \sim 100 \text{ MeV} \quad (7)$$

for  $T \sim 140$  MeV, where  $E_{\pi}$  is the typical energy of thermal pions.  $\sigma_{\pi\sigma}$  is the scattering cross section of  $\sigma$  with  $\pi$  and its value is estimated to be  $\mathcal{O}(1/f_{\pi}^2)$  from the low energy theorem. The calculated spectral function using the complex pion mass is consistent with the estimate, Eq.(7).

The smeared behavior of  $\rho_{\sigma}$  is also seen for finite density [7, 8], though the physical origin of the width is different. It is interesting to apply the prescription adopted here in the context of finite density systems.

What we have observed in this paper is expected to be universal for processes in which a particle decays into unstable particles.

## References

1. T. Hatsuda and T. Kunihiro, Phys. Rev. Lett. **55**, (1985) 158; Phys. Lett. **B185**, (1987) 304.
2. S. Chiku and T. Hatsuda, Phys. Rev. **D57**, (1998) R6, Phys. Rev. **D58**, (1998) 76001.
3. Y. Hidaka, O. Morimatsu and T. Nishikawa, Phys. Rev. **D67**, (2003) 056004.
4. P. M. Stevenson, Phys. Rev. **D23**, (1981) 2916.
5. R. G. Newton, *SCATTERING THEORY OF WAVES AND PARTICLES* (New York, USA: Springer, 1982).
6. T. Nishikawa, O. Morimatsu and Y. Hidaka, hep-ph/0302098.
7. G. Chanfray, nuc-th/0212085.
8. F. Bonutti *et al.*, CHAOS Collaboration, Nucl. Phys. **A677**, (2000) 213; Phys. Rev. Lett. **89**, (2002) 222302.